PAPER Special Section on Image Recognition and Understanding

Extraction of Finger-Vein Patterns Using Maximum Curvature Points in Image Profiles

Naoto MIURA[†a)], **Akio NAGASAKA**[†], ***and*** **Takafumi MIYATAKE**[†], ***Members***

SUMMARY A biometrics system for identifying individuals using the pattern of veins in a finger was previously proposed. The system has the advantage of being resistant to forgery because the pattern is inside a finger. Infrared light is used to capture an image of a finger that shows the vein patterns, which have various widths and brightnesses that change temporally as a result of fluctuations in the amount of blood in the vein, depending on temperature, physical conditions, etc. To robustly extract the precise details of the depicted veins, we developed a method of calculating local maximum curvatures in cross-sectional profiles of a vein image. This method can extract the centerlines of the veins consistently without being affected by the fluctuations in vein width and brightness, so its pattern matching is highly accurate. Experimental results show that our method extracted patterns robustly when vein width and brightness fluctuated, and that the equal error rate for personal identification was 0.0009%, which is much better than that of conventional methods.

key words: *finger-vein, personal identification, feature extraction, image profile*

1. Introduction

Personal identification technology is applied to a wide range of systems for functions such as area-access control and logins for PCs and E-commerce systems. Biometric techniques for personal identification, which include fingerprint [9], [10], [17], the iris [15], the voice patterns [16], facial feature [18], the hand geometry [14], the palm vein [12], or the vein on the back of the hand [13], have been notable recently because conventional means such as keys, passwords, and PIN numbers carry a risk of being stolen, lost, or forgotten.

Reliability in security and degree of convenience are very important in biometric identification systems [1]. We proposed a biometric system using finger vein-patterns, that is, patterns inside the human body [2]. This method, therefore, has the advantage of being resistant to forgery. In this system, an infrared light is transmitted from the backside of the hand. The finger is placed between the infrared light source and a camera as shown in Fig. 1. As hemoglobin in the blood absorbs the infrared light, the vein patterns on the palm side of the hand are captured as shadow patterns.

A finger image captured under infrared light contains the vein patterns which have various widths and brightness. The variation of the width of veins in the image is caused by the difference of the diameter of the vein. Furthermore, the variation of the brightness of veins is caused by the difference of transmittance of the infrared light caused by the thicknesses of finger and the amount of blood in the vein and finger. Therefore, both thin and thick vein patterns are distributed in a image, and the pattern has regions which can be seen clearly or not. Moreover, the width and brightness of the veins also fluctuate temporally because of the change of the amount of the blood in the veins and finger.

To identify a person with high accuracy requires especially extracting the pattern of the thin/thick and clear/unclear veins equally. Furthermore, the pattern extraction should be conducted with no effect of the fluctuation of the width and brightness of veins.

Conventional methods for extracting line-shaped features from images include using a matched filter [5], mathematical morphology [6], connection of emphasized edge lines [7], ridge line following for minutiae detection in grayscale fingerprint images [11] and repeating the line tracking [3], [4].

The matched filter and morphological methods can extract patterns assuming that the widths of lines are constant. Therefore, these method also emphasizes irregular shading and noises as well as the veins, and cannot emphasize the veins whose widths are narrower/wider than designed widths.

When the connection of emphasized edge lines is used to extract a finger-vein pattern, line extraction can be executed if one takes into account continuity. However, the differential operation and optimization of the line connections carry immense computational costs. Therefore, this method is not suitable for the personal identification system which requires real-time processing.

The minutiae detection algorithm for fingerprint identification is based on ridge line following. The ridge line

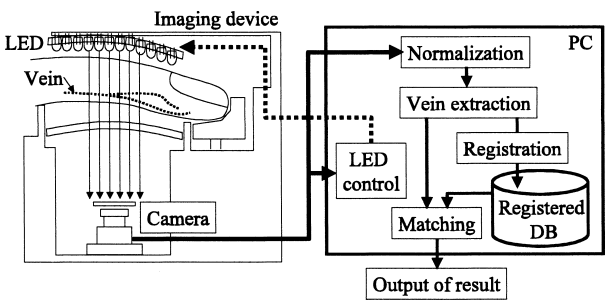

Fig. 1 Principle of personal identification using finger-vein patterns.

Manuscript received October 6, 2006.
Manuscript revised January 16, 2007.

[†]The authors are with Central Research Laboratory, Hitachi, Ltd., Kokubunji-shi, 185–8601 Japan.
a) E-mail: naoto.miura.xt@hitachi.com

DOI: 10.1093/ietisy/e90–d.8.1185

following, which is executed by checking the local darkest position in the cross-sectional profiles, works well if the ridge appears clearly. However, finger-vein images are not clear enough for this method to be used.

The repeated line tracking can extract vein patterns from unclear images. However, thin or short veins cannot be extracted adequately because the number of tracking on such veins is relatively low. Moreover, this method is tend to degrade the performance of the identification by a temporal change of widths of veins because widths of veins in a original image are faithfully reflected in widths of extracted patterns.

In this paper, we propose a method that solves these problems by checking curvature of the image profiles. Only the centerlines of veins are detected by searching for the maximum point in the curvatures of the cross-sectional profile of the vein image. These detected points are connected with each other and finally vein pattern can be obtained.

The pattern of the veins distributing in the whole image with various width and brightness can be extracted robustly by calculating the curvatures of the profile, and the pattern can be extracted robustly against the temporal fluctuation of the width of the veins by extracting only the centerlines of veins.

2. Personal Identification Using Finger-Vein Patterns

2.1 Procedure for Personal Identification

The procedure for personal identification using vein patterns in a finger is shown in Fig. 1. The detail is described below.

[Step 1] Acquisition of an infrared image of the finger with light power control

An infrared light irradiates the backside of the hand and passes through the finger. A camera located at the palm side of the hand captures the transit light. Intensity of the LED light is adjusted using the vein image such that the veins can be seen clearly.

Figure 2 (a) shows one of the prototypes for obtaining a finger image containing vein patterns. This device is designed to prevent a finger from rolling. Figure 2 (b) shows an example of a captured image.

Each captured finger images is grayscale, 240 × 180 pixels in size, with at 8 bits per pixel. The length of the finger is in the horizontal direction, and the fingertip is on the right side of the image.

[Step 2] Normalization of the image

After the image is transferred to a PC, the location, angle and scale of enlargement of the finger is normalized by using the outline of the finger. The normalization is conducted in order to realize a robust authentication against a fluctuation of a finger position which includes a distance between a finger and a camera. We assume that the three-dimensional angle of the finger such as a finger rolling can be fixed by the interface of the imaging device.

[Step 3] Vein extraction

The vein pattern is extracted from the normalized infrared image.

[Step 4] Matching

The correlation between the input pattern and each of registered patterns is calculated.

[Step 5] Output of the result of identification

When a pattern is identified in the personal identification system, the predetermined action, such as unlocking a door or logging on to a PC, can proceed.

2.2 Technical Issues

The technical issue for a high accurate personal identification is to extract the finger-vein pattern from a image under the following conditions:

(1) The veins with various widths and brightnesses are distributed in a image.

(2) The widths and brightnesses of the veins vary each trial.

The veins in the finger image have various widths, and have various brightness because the transmittance of infrared light varies according to the thickness of the finger. Figure 3 (a) shows a example of the finger-vein image. A cross-sectional profile of the image at the position of the white vertical line is shown in Fig. 3 (b). The dents in the profiles are veins. We can see that veins have various widths and brightnesses at three positions indicated by arrows. A width of a vein at the position 'A' is narrower than that of

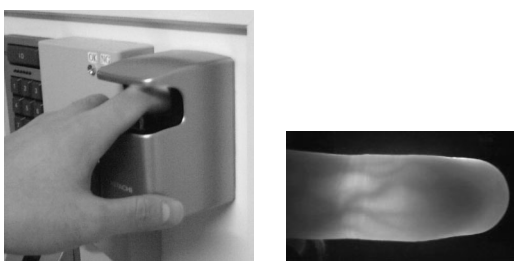

(a) Imaging device. (b) Finger-vein image.

Fig. 2 (a) Finger-vein imaging device, and (b) example of infrared finger image.

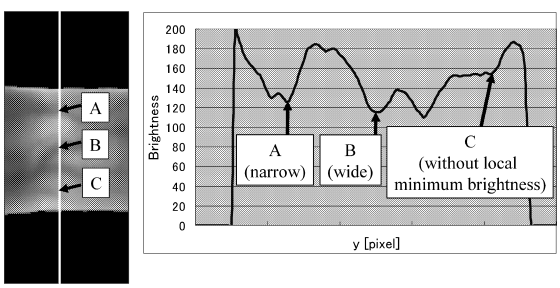

Fig. 3 Cross-sectional profile of finger-vein image.

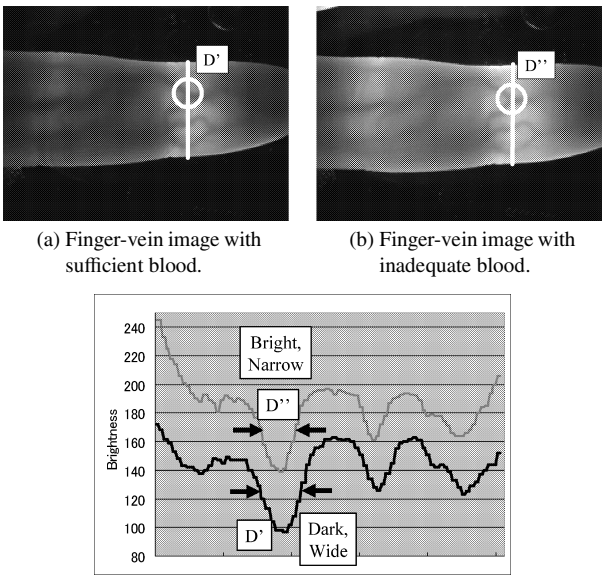

(a) Finger-vein image with sufficient blood.
(b) Finger-vein image with inadequate blood.
(c) Cross-sectional profiles of image (a) and (b).

Fig. 4 Difference of the width and brightness of veins in a image.

'B', and brightness of a vein at the position 'C' is brighter than that of 'A' and 'B'.

Furthermore, some positions of the center of a dent in the profile do not have locally minimum brightness. The cross-sectional profile of the vein at position 'C' is a dent which does not have locally minimum brightness. In this case, the center of veins cannot be obtained by detecting a local minimum point of the profile.

In addition, widths and brightnesses of veins slightly vary each trail because of a fluctuation of a volume of blood flow in a finger caused by a physical condition, change in temperature, and so on. An example is shown in Fig. 4.

Figure 4 (a) is a finger which is sufficiently filled with the blood, and (b) is a finger in which slightly less amount of the blood than (a) is flown. The veins shown in Fig. 4 (a) is thick and can be seen clearly although the average of brightness is relatively lower than (b). Compared with cross-sectional profiles of these images shown in Fig. 4 (c), the width of the vein in Fig. 4 (b) is narrower than Fig. 4 (a).

Using conventional methods, these patterns cannot be extracted easily because the veins of varied widths and brightness exist in a image. Moreover, these methods cannot extract the pattern constantly under the fluctuation of the width and brightness of the vein at each trial.

Therefore, to achieve a high accuracy requires using an algorithm that can extract all of the veins regardless of their width and brightness.

3. Extracting Finger-Vein Patterns

This section describes a new method for finger-vein extraction from finger image. First we describe the method of solving the technical issues mentioned above. Next we describe the detail algorithm.

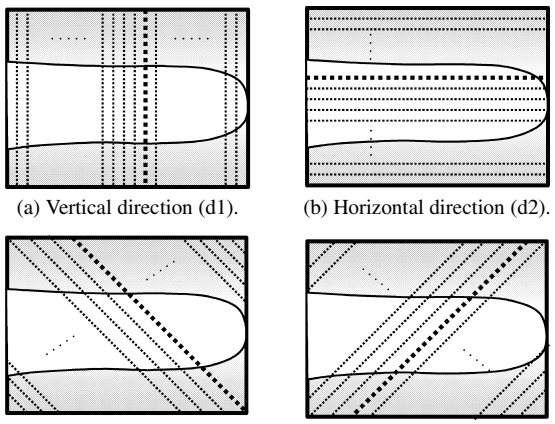

(a) Vertical direction (d1).
(b) Horizontal direction (d2).
(c) Oblique direction (1) (d3).
(d) Oblique direction (2) (d4).

Fig. 5 Direction of profiles.

3.1 Robust Vein Extraction against the Fluctuation of Its Width and Brightness

To observe the width and brightness of veins, we check a cross-sectional profile of a finger-vein image.

The cross-sectional profile around a vein appears like a dent. Many dents are the darkest than the surrounding area as shown in Figs. 3 and 4, and some dents do not have the smallest brightness in the surrounding area as shown in Fig. 3 'C'. However, the profiles around the dents have large curvature and shapes concave curve despite the widths and brightnesses of the dents.

Therefore, curvatures of the profile are calculated to detect the dents from the profile. The positions of dents have large curvature, and the center of a dent have the largest curvature around the position.

To realize a robust feature extraction against a fluctuation of the width of veins, only the positions of the center of veins are extracted.

Thus, all the center positions of the veins in the profile are detected by calculating the curvatures. This is done by analyzing the profiles, which are actually cross sections of the finger image in 4 direction (horizontal, vertical and two oblique direction intersected with horizontal and vertical direction by 45 degree, these directions are named as 'd1', 'd2', 'd3' and 'd4', see Fig. 5), and a score is assigned to each of these center points.

Finally, each point is connected to adjacent points over the whole finger image. This procedure emphasizes the line-shaped features and eliminates noises.

The advantages of our method can be described as follows:

(1) Thin/thick and dark/bright vein patterns can be obtained evenly.

(2) The noise pattern can be eliminated because only the positions of the centerlines are emphasized.

3.2 Algorithms of the Extraction of the Finger-Vein Patterns

The algorithm consists of four steps.

[Step 1] Extraction of center positions of veins
[Step 2] Connection of vein centers
[Step 3] Labeling the image

The detail algorithm is described below. F is a finger image, $F(x, y)$ is the intensity of a pixel (x, y).

[Step 1] Extraction of center positions of veins

(1) Acquisition of a profile from the image:

$P_f(z)$ is a cross-sectional profile acquired from $F(x, y)$ at vertical direction (see Fig. 5 (a)). $P_f(z)$ can be defined as follows:

$$P_f(z) = F(x, z), \tag{1}$$

where z is a position in a profile. To relate a position of $P_f(z)$ to that of $F(x, y)$, the mapping function T_{rs} is defined as $F(x, y) = T_{rs}(P_f(z))$.

(2) Calculation of the curvature of the profiles:

In general, a curvature of $f(x)$, $\kappa_f(x)$, is described as

$$\kappa_f(x) = \frac{d^2 f(x)/dx^2}{\{1 + (df(x)/dx)^2\}^{\frac{3}{2}}}. \tag{2}$$

In practice, the curvature of the discrete lines, $\kappa(z)$, can be calculated using following equations [8].

$$d_- = \frac{1}{w} \sum_{i=-w+1}^{0} \frac{y_{i-1} - y_i}{x_{i-1} - x_i} \tag{3}$$

$$d_+ = \frac{1}{w} \sum_{i=0}^{w-1} \frac{y_i - y_{i+1}}{x_i - x_{i+1}} \tag{4}$$

$$d_\pm = \frac{1}{w} \sum_{i=-w/2}^{w/2} \frac{y_i - y_{i+1}}{x_i - x_{i+1}} \tag{5}$$

$$d^2y/dz^2 = d_+ - d_- \tag{6}$$

$$dy/dz = d_\pm \tag{7}$$

$$\kappa(z) = \frac{d_+ - d_-}{\{1 + (d_\pm)^2\}^{3/2}}, \tag{8}$$

where w is width used for calculation of the average of the profile (see Fig. 6). In this study, we set at $w = 8$.

(3) Detection of the centers of veins:

The profile is classified as concave or convex depending on whether $\kappa(z)$ is positive or negative (see Fig. 7). If $\kappa(z)$ is positive, the profile $P_f(z)$ is a dent (concave).

In this step, the local maximums of $\kappa(z)$ in each concave area are calculated. The positions indicate the center positions of the veins.

The positions of these points are defined as z'_i, where $i = 0, 1, \ldots, N - 1$, and N is the number of local maximum points in the profile.

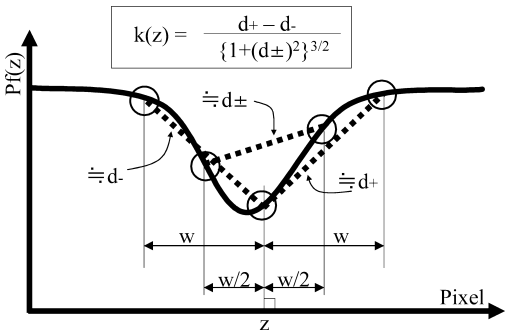

Fig. 6 Calculation of the curvature of the profile.

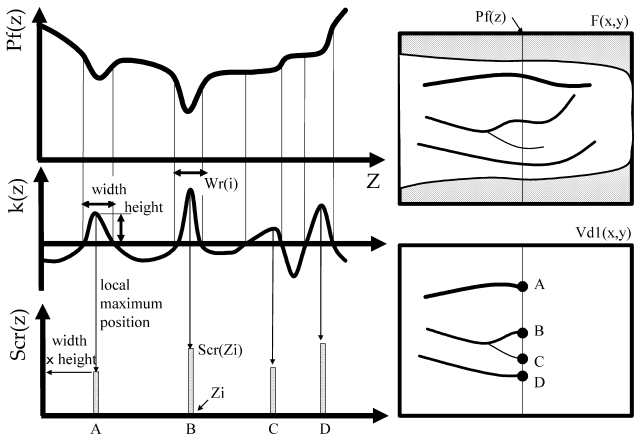

Fig. 7 Relationship among the profile, curvature and score of probability of veins.

(4) Assignment of scores to the center positions:

Scores indicating the probability that the center positions are on the veins are assigned to each center position. A score, $S_{cr}(z)$, is defined as follows:

$$S_{cr}(z'_i) = \kappa(z'_i) \times W_r(i), \tag{9}$$

where $W_r(i)$ is the width of the region where the curvature is positive and includes the z'_i (see Fig. 7).

If $W_r(i)$, which represents the width of a vein, is large, probability that it is a vein is also large. Moreover, the curvature at the center of a vein is large when it appears clearly. Therefore, the width and the curvature of regions are considered in their scores. $W_r(i)$ can be obtained at the same process of $\kappa(z)$ calculation described in step (3). It helps reduce the computational costs.

Scores are assigned to a plane $V_{d1}(x'_i, y'_i)$, where $V_{d1}(x, y)$ is a result of the emphasis of the veins by using the vertical profile of the image (V_{d1} is initialized to 0 in advance). That is,

$$V_{d1}(x'_i, y'_i) = V(x'_i, y'_i) + S_{cr}(z'_i) \tag{10}$$

where (x'_i, y'_i) represents the points defined by $F(x'_i, y'_i) = T_{rs}(P_f(z'_i))$.

(5) Calculation V_{di} using all the profiles:

To obtain the vein pattern spreading in all directions, all

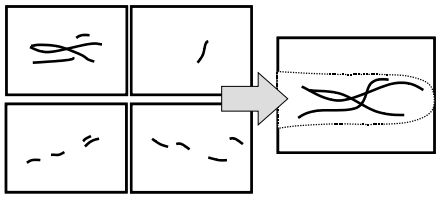

Fig. 8 Obtain the vein pattern by combining four directional vein images.

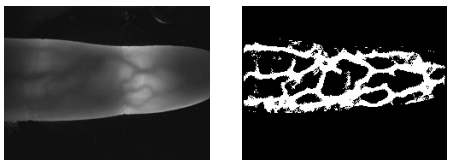

(a) Original image. (b) Extracted pattern.

Fig. 9 A sample of vein extraction result.

the profiles in four directions are analyzed. The directions used are horizontal, vertical, and the two oblique directions intersecting the horizontal and vertical at 45° as shown in Fig. 5.

A cross-sectional profile $P_f(z)$ is obtained from each direction, and the above procedure is repeatedly executed. Finally, the center positions of veins can be obtained in V_{d2}, V_{d3} and V_{d4}.

[Step 2] Connection of vein centers

To connect the centers of veins and eliminate noise, the following filter is applied to the image V_{di}.

First, a pixel (x, y) in V_{d1} and two neighboring pixels, $(x-1, y)$ and $(x+1, y)$ are checked. If these three pixels have large values, a line is drawn horizontally. When (x, y) has a small value and the neighboring pixels have large values, a line is drawn with a gap at (x, y). Therefore, the value of (x, y) should be increased to connect the line. At the same time, if (x, y) has a large value and neighboring pixels have small values, the value of (x, y) should be reduced to eliminate the noise.

This operation can be represented as follows.

$$C(x,y)_{d1} = med\{V_{d1}(x-1,y), V_{d1}(x,y), V_{d1}(x+1,y)\}, \quad (11)$$

where $med\{\ldots\}$ is a function of obtaining a median value.

Second, this calculation is made for each of the four directions in the same way, and C_{d2}, C_{d3}, C_{d4} are obtained.

Finally, a pixel value of G(x,y) is obtained by selecting the maximum of C_{d1}, C_{d2}, C_{d3} and C_{d4} for each pixe. That is, $G = \max\{C_{d1}, C_{d2}, C_{d3}, C_{d4}\}$. The extracted finger-vein pattern is stored in $G(x, y)$. Figure 8 shows the combination of four directional images.

[Step 3] Labeling the image

The vein pattern, $G(x, y)$, is binarized by using a threshold. Pixels with values smaller than the threshold are labeled as parts of the background, and those with values greater than or equal to the threshold are labeled as parts of the vein region. We determined the threshold by Otsu's method [8] such that the dispersion between the groups of values in $G(x, y)$ was maximized, assuming that the histogram of values in $G(x, y)$ was diphasic in form. We define the values of pixels labeled as parts of the background as 0 and of pixels labeled as parts of the vein regions as 255. An example of vein pattern extraction is shown in Fig. 9.

4. Experimental Results

In this section, experiments on the finger-vein extraction algorithm and their results are described. First, the robustness and accuracy of extracting the line pattern from test images is described. Second, we describe an investigation of the applicability of our identification method: an experiment using infrared finger images from 678 volunteers. In this experiment, the finger images were captured using a grayscale, infrared-sensitive 1/2-in. CCD camera (NC300AIR, TAKEX). The resolution of the images was approximately 0.3 mm/pixel.

For comparison, three methods (proposed method, the line tracking method, and the matched filter method) were evaluated in the experiments.

The matched filter method uses two-dimensional filters [4], [5]. The filters are designed so that their profiles match the cross-sectional profiles of typical veins. The filters consist of four filter kernels, with each filter rotated to optimize for a different angular vein direction. Figure 10 shows one of the filter kernels. Each filter is convoluted to the captured image independently, and all convolution values are added together.

The line tracking method tracks veins repeatedly, and the tracking starts at various positions [3], [4]. A line is tracked by moving pixel by pixel along the veins, checking the cross-sectional profiles of the image. When a dark line is not detected, a new tracking operation starts at another position. This operation is executed repeatedly. Finally, the loci of the lines overlap, and the finger-vein pattern is obtained statistically.

4.1 Robustness and Accuracy of the Pattern Extraction Using Test Images

To evaluate the robustness and accuracy of line extraction, a line pattern extraction from test images was conducted. The test images which had vein-like patterns were made artificially.

The experiment was conducted as follows.

(1) Creation of test images
(2) Extraction of the line pattern
(3) Evaluation of the following accuracy
  (A) Accuracy of the pattern extraction
  (B) Robustness of vein width and brightness fluctuation

The detail of the experiment is described below.

4.1.1 Creation of Test Images

Figure 11 shows a procedure of creating test images. The procedure consists of four steps:

[Step 1] Create a vein-like pattern

Firstly, lines which look like vein patterns was drawn by hand (Fig. 11 (a)). The pattern consists of thin lines and it is binary image.

Secondly, vein patterns which have various widths and brightnesses were created based on the thin lines. The curve of the cross-sectional profile is assumed the Gaussian function (see Fig. 11 (b)).

To include the various widths and brightness in a image, The vein-like pattern is created under the following conditions:

(A) The width is gradually larger as the position is toward left side of the image.

(B) The brightness is gradually darker as the position is toward the upper side of the image.

An example of the vein pattern is shown in Fig. 11 (c). This image is 8 bit gray scale, 240×180 in size. The widest width of vein is 28×2 pixels at the left side of the image, and the narrowest width of vein is 1 pixel at the right side of the image.

[Step 2] Create vein-like patterns with various widths

In this step, 32 vein patterns which had different average line width were created based on the vein-like pattern created in step1.

Each pattern had a different average line width, ranging from 100% (normal width) to 200% (large width). We call these percentages 'width ratios'. We assume that the width ratio of the vein-like pattern created in step 1 is 100% (see Fig. 12 (a)).

26	8	-18	-32	-18	8	26
26	8	-18	-32	-18	8	26
26	8	-18	-32	-18	8	26
26	8	-18	-32	-18	8	26
26	8	-18	-32	-18	8	26
26	8	-18	-32	-18	8	26
26	8	-18	-32	-18	8	26

Fig. 10 Matched filter kernel.

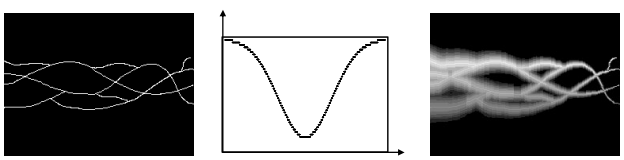

(a) Hand written pattern. (b) Gaussian function. (c) Created vein pattern.

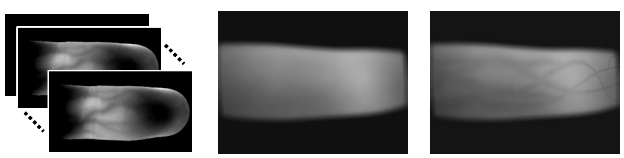

(d) Finger-vein images. (e) Average image. (f) Created finger-vein image.

Fig. 11 Procedure of creation of the test images.

[Step 3] Create a background of the finger image

To create a background of a finger-vein image, an average image of genuine finger-vein images was calculated (see Fig. 11 (d)). The images contain about 100 finger images, each finger had similar finger width. After that, 9×9 average filter is applied to obtain the average image. The image is shown in Fig. 11 (e).

[Step 4] Combine the vein patterns and background of the finger

To create a test image $F_t(x, y)$, the created vein images was combined to the average image using following equation.

$$F_t(x, y) = V_t(x, y) - B_t(x, y) \times 16/255 \quad (12)$$

where $V_t(x, y)$ is the vein-like pattern, $B_x(x, y)$ is the background image. An example of the test image is shown in Fig. 11 (f). In this step, 32 test images were created using 32 vein patterns created in step 2 (see Fig. 12).

4.1.2 Accuracy of the Pattern Extraction

To evaluate the accuracy of the pattern extraction of the various widths and brightnesses of lines, a pattern extraction from test image which contains various widths and brightnesses of lines was executed.

To evaluate an accuracy of line detection, original hand-written pattern and extracted pattern were compared.

The evaluation was conducted by the template matching method. That is, two binary images are overlapped and compared each pixel value of two images.

When line patterns did not exist in the extracted image where line patterns exist in the original image, the extraction was not sufficiently conducted. The ratio of these matter is named "undetection rate".

In a similar way, when line patterns exist in the extracted image where line patterns did not exist in the original image, the extraction was not precisely conducted. The

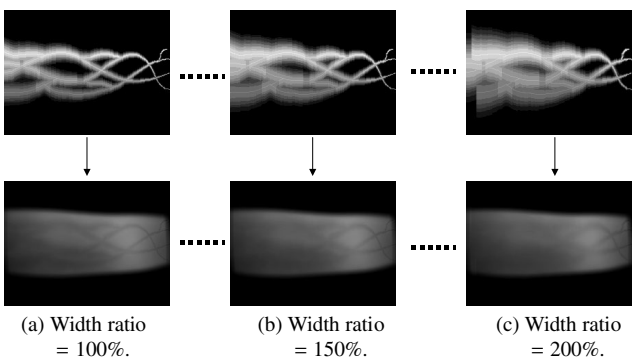

(a) Width ratio = 100%. (b) Width ratio = 150%. (c) Width ratio = 200%.

Fig. 12 Examples of the test images which have various average of the width.

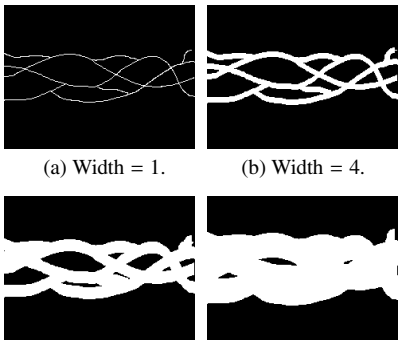

(a) Width = 1. (b) Width = 4.

(c) Width = 8. (d) Width = 16.

Fig. 13 Examples of mask patterns used for calculating the false/undetection rate.

ratio of these matter is named "false detection rate". If these error rates were small, the algorithm had a high-accuracy of the pattern extraction.

The experiment was conducted following procedure.

[Step 1] Extraction of the pattern

The pattern was extract from the test image whose width ratio = 100%.

[Step 2] Creation of the mask patterns

We used mask patterns which had various width of line patterns for calculating false detection/undetection ratios.

When the original hand-written pattern and extracted pattern are compared by the template matching, false detection rate or/and undetection rate become larger if the widths of the extracted patterns are different from those of original patterns. However, each algorithm does not always recreate the width of veins faithfully. That is, each algorithm has different condition for extraction of the veins concerning the width of the pattern.

To conduct fairly evaluation of these rates under the condition, the original pattern was convert to the mask patterns which had various width. After that, each mask pattern was compared with a patten extracted by an algorithm. Finally, false detection/undetection rates were calculated using all the masks.

These masks include 16 different width patterns and each mask has a constant width. Figure 13 shows these masks. The narrowest width is 1 pixel (Fig. 13 (a)), and the widest width is 16×2 pixels (Fig. 13 (d)).

[Step 3] Calculating of undetection rate and false detection rate

Using one of the mask pattern $M_i(x, y)$ $(i = 1, 2, 3, \ldots, 16)$, undetection rate $R_u(i)$ and false detection rate $R_f(i)$ are calculated using following equations.

$$R_u(i) = \frac{\sum_{\forall(x,y)}\{T_r(M_i(x,y) = 255 \wedge V_e(x,y) = 0)\}}{\sum_{\forall(x,y)}\{T_r(M_i(x,y) = 255)\}} \quad (13)$$

$$R_f(i) = \frac{\sum_{\forall(x,y)}\{T_r(V_e(x,y) = 255 \wedge M_i(x,y) = 0)\}}{\sum_{\forall(x,y)}\{T_r(V_e(x,y) = 255)\}} \quad (14)$$

where $V_e(x, y)$ is extracted vein pattern from the test image, T_r is a function such that if logical expression b is true, $T_r(b)$ is 1, if otherwise, $T_r(b)$ is 0.

These rates are calculate by using all mask patterns i.

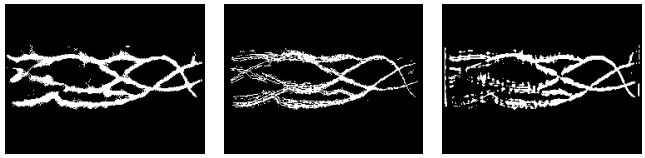

(a) Proposed. (b) Line tracking. (c) Matched filter.

Fig. 14 Result of the pattern extraction using each method.

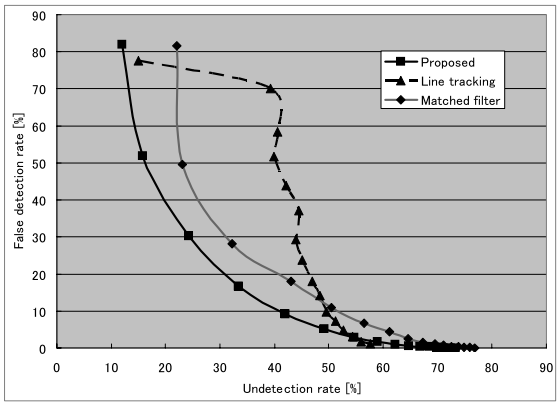

Fig. 15 Result of the accuracy of the extraction of the pattern.

[Step 4] Obtention of the accuracy of pattern extraction

A set of undetected rate and false detection rate is obtained using a mask pattern. To obtain the relationship between two error rates as the receive operation characteristic (ROC) curve, $R_u(i)$ $(i = 1, 2, \ldots, 16)$ and $R_f(i)$ $(i = 1, 2, \ldots, 16)$ are plotted to vertical axis and horizontal axis, respectively.

The patterns extracted from the test image using each method are shown in Fig. 14. The pattern extracted by the proposed method (Fig. 14 (a)) was relatively clear. On the other hand, the pattern in (b) and (c) were unclear where the line width of the original pattern was relatively wide.

The results of calculating false detection/undetection rate were shown in Fig. 15 as ROC curve. When the width of the mask pattern was getting larger, the false detection rate was getting smaller and the undetection rate was getting larger at the same time. Both false detection rate and undetection rate obtained by the proposed method was lower than that by other methods at most of the plotting points. Equal error rates of the curves were 26%, 42% and 31% obtained by proposed, line tracking and matched filter methods, respectively. The results showed the proposed method can realize an accurate extraction.

4.1.3 Robustness against Fluctuation of Width of Lines

On the assumption that the widths of veins vary each trial, patterns extracted from artificial test images which had same pattern and different width of lines were obtained and compared.

The experiment was conducted as follows.

[Step 1] Extraction of the vein patterns from test images

The patterns were extracted from 32 test images shown as Fig. 12. Each image contains various average of width.

[Step 2] Calculation of the correlation among the patterns

All extracted patterns were compared with each other. To calculate a correlation of two patterns, we defined a mismatch ratio [4].

First, a binarized vein image is converted into three categories: Vein, Background, and Ambiguous.

Second, two converted patterns are overlapped with each other. The values of overlapping pixels are compared pixel by pixel. The paris of pixels, where one is a Vein and the other a Background pixel, are counted in entire image. Such a pair is called a mismatch.

After that, the smallest number of mismatched pair is searched moving the positions of the overlap.

The ratio of the smallest number of mismatched pairs to the total number of Vein pixels is defined as the mismatch ratio, and it quantifies the differences of two patterns.

The results of creation of the matching data were shown in Fig. 16. The patterns are clearly extracted using each method if the width ratio is 100%. Using the proposed method, the patterns are clearly extracted even if the width ratio is 200% (see Fig. 16 (a) (b) (c)). On the other hand, the patterns obtained from the original test image have slightly unclear lines by using the other methods. Especially, as the width ratio was getting larger, the pattern was getting much unclear.

To estimate the fluctuation quantitatively, the transition of mismatch ratio was calculated. Each pattern obtained from original test image with various line width was compared with a pattern whose width ratio was 150% and mismatch ratios were calculated. This evaluation can estimate the robustness of the fluctuation of the vein widths.

The results are shown in Fig. 17. When the width rate was away from 150%, mismatch ratio was getting larger. The mismatch ratio of our method was 2.83% on average. The line tracking and the matched filter methods had the mismatch ratio averages of 4.62% and 4.56%. The mismatch ratio of our method stayed low even when the widths of the patterns were changed. Therefore, the pattern matching of our method is robust against vein width and brightness fluctuations.

4.2 Personal Identification Using Finger-Vein Patterns

To examine the personal identification performance by using the proposed method, we did an experiment to identify a large number of patterns. The experiment includes an equal error rate (EER) evaluation, where a false accept rate (FAR) equals a false reject rate (FRR), of a dataset of infrared finger images.

The dataset contained 678 different finger images and two images per finger were stored. They were obtained from people working in our laboratory, ranging in age from 20s to 40s and approximately 70% men. Two images were captured on the same day and the second image was captured with a retry about 30 seconds after the first capturing.

The FRR was obtained by calculating the mismatch ratios using both images of each finger, and the FAR was obtained by calculating the mismatch ratios among the images of different fingers for all combinations (678×677). All the method mentioned above were independently evaluated in the same way.

To make a comparison of the accuracy among three methods, we calculated the EER of each method. Because the FRR and FAR are discrete numbers, EER such that FAR = FRR dose not always exist. Therefore, we defined the approximate EER, that is, EER is defined as FAR where |FAR − FRR| is minimized. FAR can represent more detailed accuracy than FRR because the number of data used for calculating FAR is much larger than that of FRR. The minimum value of |FAR − FRR| can be searched by varying the threshold of mismatch ratio which is defined as a boundary between same finger and different finger.

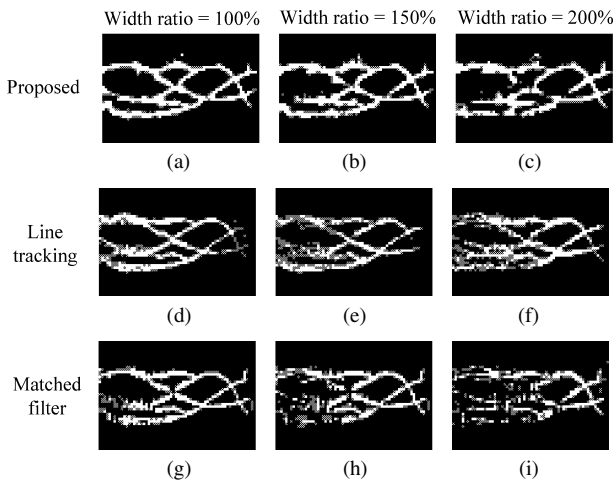

Fig. 16 Matching data obtained from various width ratio.

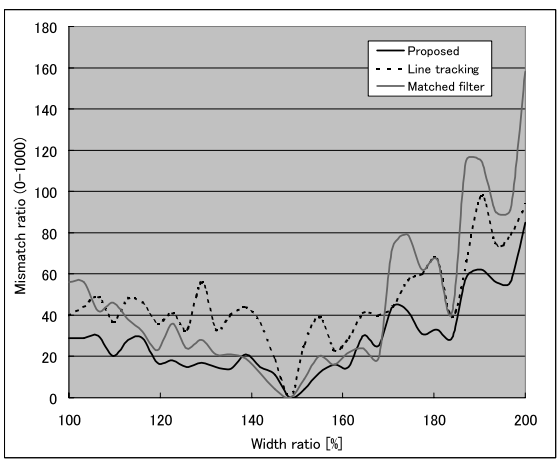

Fig. 17 Transition of the mismatch ratio based on the matching data obtained the test image whose width ratio = 150%.

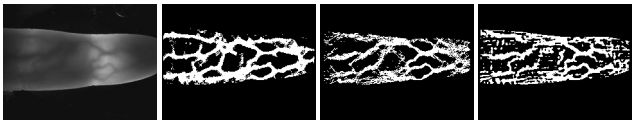

(a) Original image. (b) Proposed. (c) Line tracking. (d) Matched filter.

Fig. 18 Example of the vein pattern extracted from real finger-vein image.

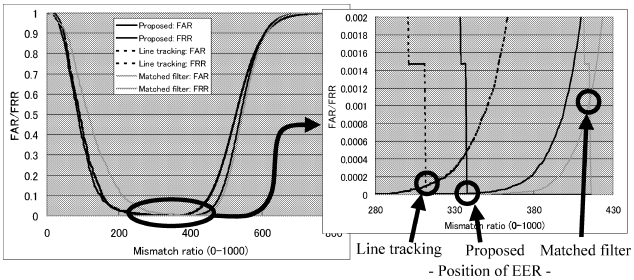

Fig. 19 Relationship between FAR and FRR.

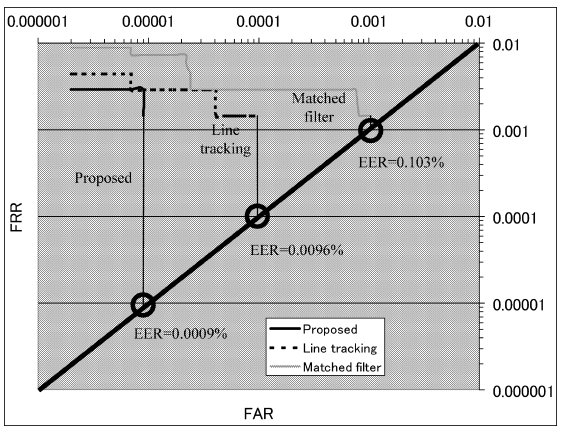

Fig. 20 ROC curve and EER.

Table 1 EER for personal identification.

methods	proposed	line tracking	matched filter
EER	0.0009%	0.0096%	0.103%

Figure 18 shows examples of extracted vein images using each method. The pattern using the proposed method was relatively clearer than the others.

The results of calculating the mismatch ratio is shown in Fig. 19. The positions of EER were slightly different from each other at each method.

The receive operation characteristic (ROC) curve, which shows the relationship between FAR and FRR, is shown in Fig. 20. EER can be obtained from Fig. 20 as shown in Table 1.

The EER of the proposed method was 0.0009%. On the other hand, the EER using the repeated line tracking method was 0.0096% and the EER of the matched filter method was 0.103%. This shows that the error rate in personal identification is smaller for the proposed method than for the conventional methods. Thus, the finger vein identification based on our approach is much effective.

5. Conclusion

We proposed a method of extracting vein patterns. To precisely extract patterns from vein images with various widths and brightnesses, the centerlines of the veins are extracted by calculating the curvature of the cross-sectional profile of the image.

An evaluation of the robustness of our method against fluctuations in widths and brightnesses of veins showed that it is far superior to the conventional methods. A further experiment showed that the EER is 0.0009%, which means the proposed method is much better than that of conventional methods.

We plan to apply the system to many areas which require personal identification. More specifically, we will work on development of small device. To apply it to small items such as a notebook computer, a cell phone and so on, we plan to design small interface, light weight algorithm for image processing.

Acknowledgments

We thank all the members of Hitachi CRL who allowed us to take infrared images of their fingers.

References

[1] W. Shen, M. Surette, and R. Khanna, "Evaluation of automated biometrics-based identification and verification systems," Special Issue on Automated Biometric Systems, Proc. IEEE, vol.85, no.9, pp.1463–1478, 1997.
[2] M. Kono, H. Ueki, and S. Umemura, "A new method for the identification of individuals by using of vein pattern matching of a finger," Proc. Fifth Symposium on Pattern Measurement, pp.9–12, Yamaguchi, Japan, 2000.
[3] N. Miura, A. Nagasaka, and T. Miyatake, "An extraction of finger vein patterns based on multipoint iterative line tracing," Proc. IEICE Gen. Conf. 2001, D-12-4, 2001.
[4] N. Miura, A. Nagasaka, and T. Miyatake, "Automatic feature extraction from non-uniform finger vein image and its application to personal identification," Proc. MVA2002, pp.253–256, Nara, Japan, IAPR, 2002.
[5] A. Hoover, V. Kouznetsova, and M. Goldbaum, "Locating blood vessels in retinal image by piece-wise threshold probing of a matched filter response," IEEE Trans. Med. Imaging, vol.19, no.3, pp.203–210, 2000.
[6] T. Walter, J. Klein, P. Massin, and F. Zana, "Automatic segmentation and registration of retinal fluorescein angiographies — Application to diabetic retinopathy," First International Workshop on Computer Assisted Fundus Image Analysis, pp.15–20, Copenhagen, Denmark, May 2000.
[7] P. Montesinos and L. Alquier, "Perceptual organization of thin networks with active contour functions applied to medical and aerial images," ICPR'96, pp.647–651, Vienne, Autriche, 1996.
[8] M. Nagao, Methods of Image Pattern Recognition, Corona Publishing, 1983.
[9] A.K. Jain and S. Pankanti, "Automated fingerprint identification and imaging systems," in Advances in Fingerprint Technology, 2nd ed., ed. H.C. Lee and R.E. Gaensslen, Elsevier Science, New York, 2001.

[10] S. Prabhakar, A.K. Jain, and S. Pankanti, "Learning fingerprint minutiae and type," Pattern Recognit., vol.36, pp.1847–1857, 2003.
[11] D. Maio and D. Maltoni, "Direct gray-scale minutiae detection in fingerprints," IEEE Trans. Pattern Anal. Mach. Intell., vol.19, no.1, pp.27–40, Jan. 1997.
[12] http://jp.fujitsu.com/group/labs/
[13] S. Im, H. Park, Y. Kim, S. Han, S. Kim, C. Kang, and C. Chung, "A biometric identification system by extracting hand vein patterns," Journal of the Korean Physical Society, vol.28, no.3, pp.268–272, March 2001.
[14] A.K. Jain, A. Ross, and S. Pankanti, "A prototype hand geometry-based verification system," Proc. 2nd Int'l Conference on Audio- and Video-based Biometric Person Authentication, pp.166–171, Washington D.C., March 1999.
[15] W.W. Boles and B. Boashash, "A human identification technique using images of the iris and wavelet transform," IEEE Trans. Signal Process., vol.46, no.4, pp.1185–1188, April 1998.
[16] G.K. Venayagamoorthy, V. Moonasar, and K. Sandrasegaran, "Voice recognition using neural networks," Proc. IEEE South African Symposium on Communication and Signal Processing (COMSIG 98), pp.29–32, Sept. 1998.
[17] W. Zhang and Y. Wang, "Core-based structure matching algorithm of fingerprint verification," IEEE Proc. International Conference on Pattern Recognition, vol.1, pp.70–74, Aug. 2002.
[18] X. Chen, P.J. Flynn, and K.W. Bower, "Visible-light and infrared face recognition," Proc. Workshop on Multimodal User Authentication, pp.48–55, Dec. 2003.

Naoto Miura received B.E. and M.E. degrees from the University of Tokyo, Japan, in 1998 and 2000, respectively. Since 2000 he has been with the Central Research Laboratory of Hitachi Ltd. and is presently a researcher in the Intelligent Media Systems Research Department. His research interests include biometric identification, image processing, and pattern recognition.

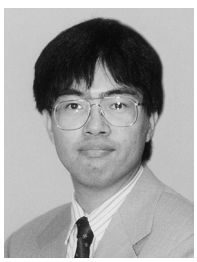

Akio Nagasaka received B.E. and M.E. degrees from Hokkaido University, Japan, in 1989 and 1991, respectively. He joined the Central Research Laboratory of Hitachi Ltd. in 1991 and is presently a Senior Researcher in the Intelligent Media Systems Research Department. He has been active in the fields of real-time video-image processing, multimedia systems, and biometrics. He received a Doctoral Degree in Electronics and Information Engineering from Hokkaido University in 2000. He has also been a Visiting Associate Professor at the Japan Advanced Institute of Science and Technology since 2001.

Takafumi Miyatake graduated from Tadotsu Technical High School, Kagawa, Japan, in 1971, and from Hitachi Technical College, Kanagawa, Japan, in 1973. Since 1971 he has been with the Central Research Laboratory of Hitachi Ltd. and is presently a Chief Researcher in the Intelligent Media Systems Research Department. He has participated in R&D activities in the fields of 3D object recognition, drawing recognition, and real-time video analysis; his current interest is extended image processing for security systems. From 1981 to 1982 he was a Visiting Researcher at Kyoto University, Kyoto, Japan. He received a Doctoral Degree in Information Engineering from the University of Tokyo in 1996. He is a Member of The Institute of Image Information and Television Engineers, Tokyo, Japan.